Guided Wave Testing

Paul Fromme

p.fromme@ucl.ac.uk

Department of Mechanical Engineering, UCL

London, UK

Abstract

Guided waves can propagate long distances in thin-walled structures, such as pipelines or plates. This allows for the efficient monitoring and testing of large structures, and for the detection of hidden or inaccessible defects. Guided wave propagation is dispersive and multi-modal, requiring a thorough understanding of the wave propagation and scattering phenomena from simulations. Guided wave dispersion diagrams, mode shapes and typical signals are illustrated for the example of isotropic plates. Both low and high frequency guided waves have been used for the testing of plate structures, with different wave modes and applications including tomography and arrays for the detection and localization of defects. For multi-layered and anisotropic structures, guided wave propagation becomes more complex, and often the fundamental guided wave modes are employed for defect detection. For pipelines different commercially available testing systems have been developed and long propagation distances up to 100 meters have been achieved. Careful selection of guided wave mode and excitation frequency allow the minimization of attenuation due to viscoelastic coatings and in buried pipelines. Synthetic focusing using non-axisymmetric modes improves defect imaging and localization. Experimental methods differ from standard ultrasonic testing, as good control of the excited guided wave mode shape and signal are required to achieve improved sensitivity for small defects. In addition to contact piezoelectric transducers, electromagnetic and laser techniques allow for noncontact measurements. Finite Element Analysis is one of the numerical simulation techniques used to obtain a better understanding of guided wave testing and to improve defect characterization.

1. Introduction

Increasingly guided waves are employed for non-destructive testing (NDT) and structural health monitoring (SHM) applications, as they offer capabilities for the testing of large structures and detection of hidden or inaccessible defects. For structures that are thin in at least one dimension, such as plates and pipes, through multiple reflections in the thickness direction, standing wave modes can develop that can propagate over long distances with limited amplitude loss (Cawley, Lowe et al. (2003). Commercially successful equipment has been developed by a number of manufacturers for the testing of pipes (Rose 2002), (Mudge 2001), (Alleyne, Jones et al. 2017), where defects can been detected at distances up to 100 meters.

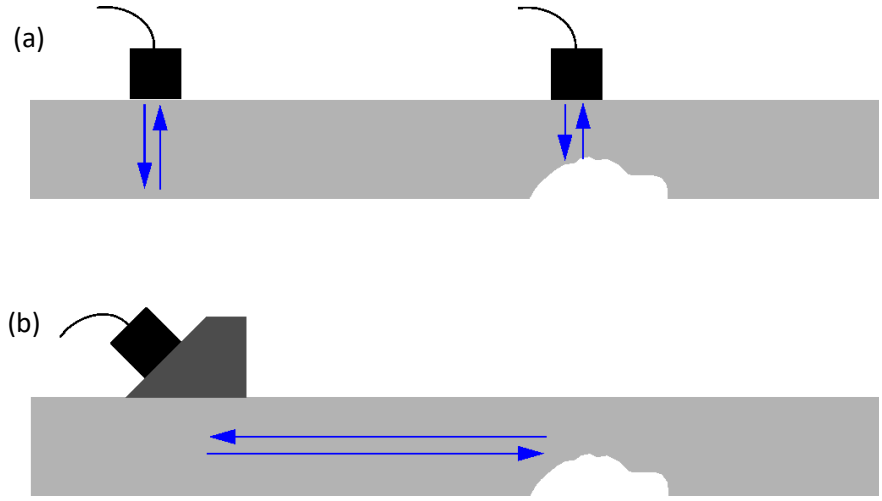

Figure 1. Schematic of a) bulk ultrasonic and b) guided wave testing.

Compared to conventional bulk ultrasonic testing, the wave propagation direction is along the structure rather than through the thickness (Fig. 1), reducing the requirement for scanning and offering the potential to inspect structures with limited access, such as buried or coated pipelines (Rose 2014). Increasingly, permanently installed sensors are employed, allowing a monitoring rather than inspection approach to reduce variations between successive measurements and improve the sensitivity for defect detection.

However, there is typically a balance between the ability to cover a large area from a single sensor location and the sensitivity for the detection of small defects. Applications for large structures require lower frequencies to achieve long wave propagation distances, with the large wavelength corresponding to a reduced sensitivity for small defects. Often guided waves are used in a screening mode to identify potentially damaged areas and provide a preliminary assessment of the damage severity, rather than a detailed defect characterization and sizing.

While providing many benefits, it must be understood that guided wave propagation is more complex than for bulk ultrasonic waves and depends both on the geometry and excitation frequency. Multiple wave modes can propagate in the structure and the propagation velocity depends on the excitation frequency. This dispersion and the resulting pulse distortion requires a good understanding of the wave propagation and control of the wave excitation to ensure reliable defect detection. This has been recognized by the international norms for guided wave testing (e.g. BS 9690-1:2011, ASTM E2775 - 16) and necessitates improved training to provide reliable testing results.

This chapter aims to provide an overview of guided waves for non-destructive testing. Section 2 explains some of the important phenomena in more detail (for the example of plates), to provide a better understanding of the application, benefits, and limitations of guided wave testing. Application examples are discussed in section 3 for isotropic and anisotropic (composite) plates, as well as bonded, multi-layered, and curved structures. Section 4 gives an overview of applications for pipes, with a focus on how the choices for wave modes influence both the defect detection sensitivity and experimental and processing requirements. Sections 5 and 6 provide a brief discussion of experimental and simulation methods for guided wave testing.

2. Guided Wave Propagation

Guided waves can propagate along plates, with multiple modes and varying directionality. Conceptually this can be understood either as the constructive interference of multiple bulk ultrasonic waves reflected and mode converted through the thickness of the structure, or as guided wave modes through the thickness. Both conceptual derivations result in identical equations, which for the case of a plane wave front in an isotropic, homogeneous plate, can be described by the classical Rayleigh-Lamb theory.

$$\frac{\tan(qh)}{\tan(ph)} = -\frac{4k^2pq}{(q^2-k^2)^2} \quad \text{Symmetric Lamb wave modes} \qquad \text{(Eq. 1)}$$

$$\frac{\tan(qh)}{\tan(ph)} = -\frac{(q^2-k^2)^2}{4k^2pq} \quad \text{Anti-symmetric Lamb wave modes} \qquad \text{(Eq. 2)}$$

where $p^2 = \left(\frac{\omega}{c_L}\right)^2 - k^2$ and $q^2 = \left(\frac{\omega}{c_T}\right)^2 - k^2$

with plate thickness $2h$, angular frequency ω, wavenumber k, longitudinal wave velocity c_L and shear wave velocity c_T.

These equations and the wave propagation have been widely described and discussed in the seminal work by (Achenbach 1973), (Auld 1973), (Graff 1975), (Rose 2014), and (Viktorov 1967). For the simple case of a uniform plate, an analytical solution is possible. For more complex structures, numerical methods such as SAFE (semi-analytical finite element) analysis (Predoi, Castaings et al. 2007) or semi-analytical approaches such as the global matrix approach employed in the Disperse software (Pavlakovic, Lowe et al. 1997) have been demonstrated to be numerically stable and efficient. Figure 2 shows the dispersion curves for an aluminum plate calculated using the Disperse software.

Figure 2a shows the phase velocity for the different wave modes for variation of the frequency-thickness product, as the wave speed depends on this product. The corresponding group velocities (the speed of the wave pulse) are shown in Fig. 2b. For higher frequency-thickness products multiple wave modes can propagate, above the cut-off frequencies of the higher wave modes.

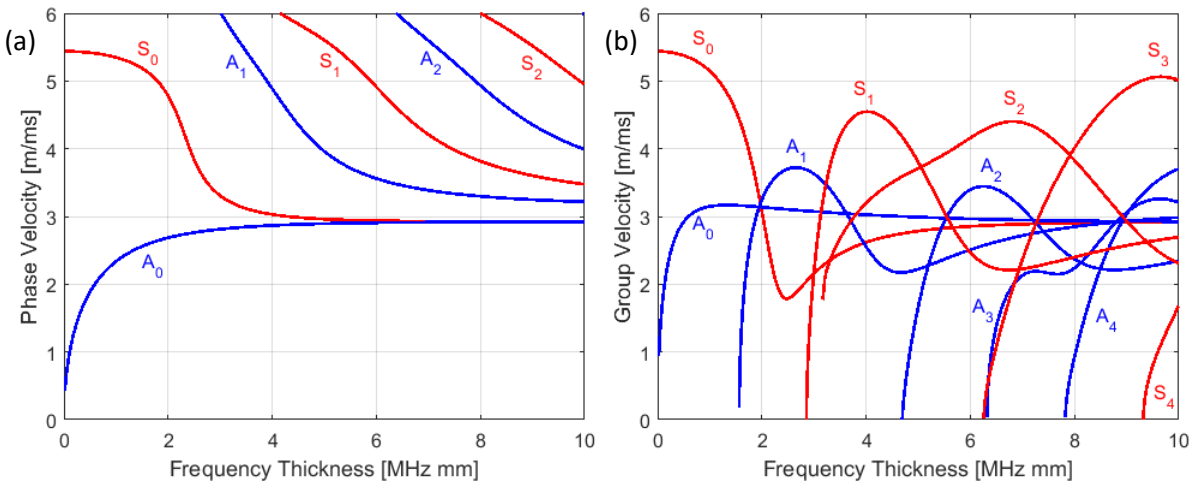

Figure 2. Dispersion diagram for aluminum plate; a) phase velocity; b) group velocity.

At the cut-off frequencies the respective group velocity of that wave mode tends towards zero, while the phase velocity tends towards infinity. Essentially, at the cut-off frequency this can be thought of as a standing wave mode or vibration across the plate thickness. Below the cut-off frequencies of the higher wave modes, only the two fundamental wave modes can propagate. The first anti-symmetric wave mode A_0 can be considered similar to a bending or flexural wave at low frequency-thickness, with large out-of-plane displacement and smaller, anti-symmetric in-plane motion, as shown in Fig. 3a. At low frequencies the first symmetric Lamb mode S_0 resembles a longitudinal wave with large, symmetric in-plane displacement (Fig. 3b) and very limited dispersion, i.e. the phase and group velocity are reasonably constant and similar to a bulk, longitudinal ultrasonic wave.

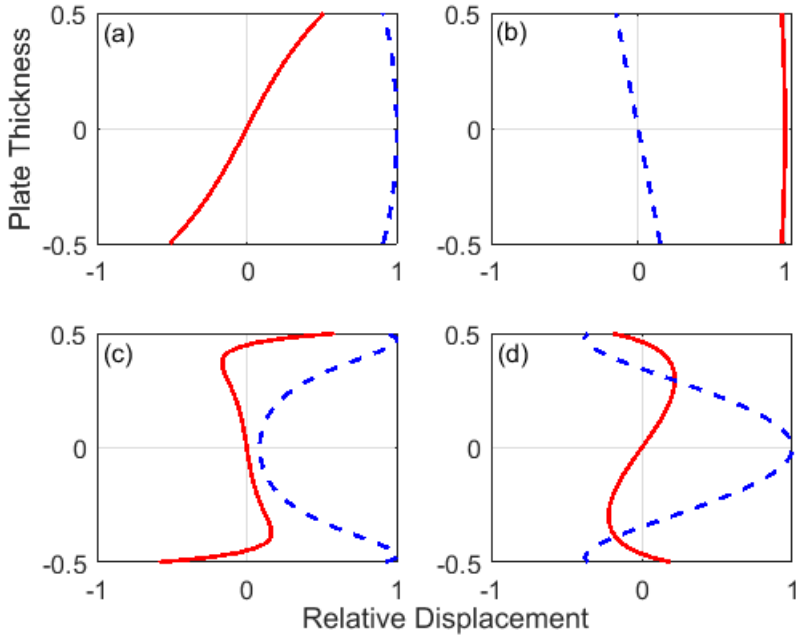

Figure 3. Guided wave mode shapes; a) A_0 mode at 0.5 MHz mm; b) S_0 mode at 0.5 MHz mm; c) A_0 mode at 10 MHz mm; d) A_1 mode at 10 MHz mm; solid: in-plane displacement; dashed: out-of-plane displacement.

For high frequency-thickness products the fundamental S_0 and A_0 Lamb wave modes tend towards the Rayleigh surface wave velocity with similar mode shapes through the thickness (Fig. 3c), while the higher Lamb wave (Fig. 3d) modes tend towards the shear velocity.

The complexity of the guided wave propagation requires different considerations as compared to conventional bulk ultrasonic wave testing. Dispersion, the fact that different frequency components within a wave packet propagate at different velocities, leads to changes in the pulse shape and makes some of the standard UT evaluation (e.g. based on pulse shape) difficult. Furthermore, the variation in group velocity with frequency leads to pulse distortion, the spreading in time of the energy contained within a wave pulse. This reduction in amplitude with propagation distance was one of the most relevant problems encountered during early stages of guided wave testing (Alleyne and Cawley 1991). Instead of the conventional short duration, wide frequency range pulse employed in standard ultrasonic testing in combination with resonant transducers, different excitation signals are often employed for guided wave testing.

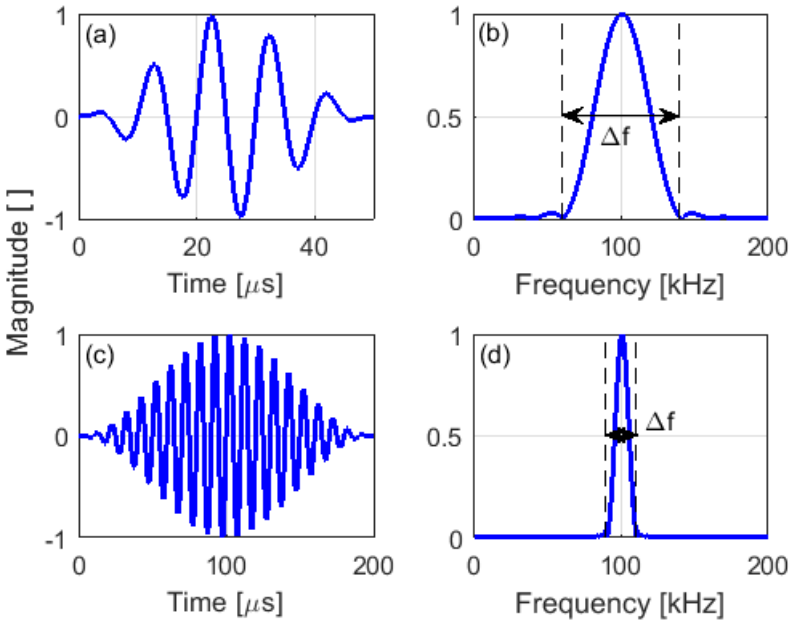

Figure 4. 5 cycle sinusoid (100 kHz center frequency) in Hanning window: a) time signal, b) frequency content; 20 cycle sinusoid in Hanning window: c) time signal, d) frequency content.

In order to achieve a narrow frequency bandwidth to limit dispersion and pulse distortion, tone bursts such as 5 cycles of a sinusoid in a Hanning window have been found beneficial (Fig. 4a/b).

$\Delta f = \frac{4}{N} f$ with center frequency f (Eq. 3)

The number of cycles *N* controls the trade-off between pulse length and frequency bandwidth Δf (Eq. 3), so a 20 cycle toneburst (Fig. 4c/d) has a longer time duration but narrower frequency bandwidth than a 5 cycle pulse (Fig. 4a/b). Another approach has been to use a wideband excitation such as a chirp signal, and to post-process the measured time traces by convolution with narrowband signals to isolate specific frequencies within the bandwidth of the excitation (Michaels, Lee et al. 2013). In order to achieve this control of the excitation signal, typically different equipment compared to standard ultrasonic pulser/receivers is required, such as arbitrary function generators to generate the desired time signals, and wide-band amplifiers to achieve acceptable signal-to-noise (SNR) ratios. This will be discussed further in section 5 dealing with experimental methods.

Another important consideration is that signals containing multiple wave modes propagating at different speeds can be quite difficult to analyze (Alleyne and Cawley 1991), thus often selective excitation of Lamb wave modes is desired. This is reasonably straight-forward to achieve for the fundamental wave modes below the cut-off frequencies of the higher wave modes. The S_0 wave mode has been widely employed as it is non-dispersive at low frequencies, its modeshape and displacement are similar to longitudinal bulk ultrasonic waves (Fig. 3b), and it has the highest group velocity, thus is easily identified as the first arrival pulse. The wave mode has some limited dispersion around 0.5 MHz mm, which has been used for tomography to detect and localize plate thinning (Leonard, Malyarenko et al. 2002). Disadvantages of the S_0 mode at low frequency thickness products are the rather large wavelength and limited sensitivity for some defects in composite structures (Guo and Cawley 1993), but compared to

the A_0 mode it has the advantage of limited attenuation for water loading. In contrast the A_0 wave mode is dispersive at low frequencies, but limited pulse distortion was found around 0.5 MHz mm for steel and aluminum plates. Together with the shorter wavelength this allows for good defect detection sensitivity (Fromme, Wilcox et al. 2006). At higher frequency-thickness products the selective mode excitation requires better experimental configuration and good understanding of the guided wave propagation and attenuation characteristics.

3. Guided Wave Testing of Plate Structures

3.1 Defect detection in isotropic (metal) plates

Guided waves can quickly interrogate large plate and shell structures and have sensitivity for the detection of surface and subsurface features (Rose 2002). Guided waves propagate in two dimensions along thin structures, making it necessary to achieve a distinction between the different Lamb wave modes and to take the two-dimensional spreading of the guided ultrasonic wave into account. The angular resolution of any monitoring device has to be sufficient to distinguish between different features. The amplitude of the guided wave decreases with distance, as the energy spreads over a larger area. Therefore, a sufficiently large dynamic range is required for the detection of small defects in the presence of structural features. In order to simplify the signal processing, most non-destructive testing applications work in the low frequency-thickness regime below the cut-off frequencies of the higher wave modes, where only three guided wave modes (S_0, A_0, SH_0) can exist.

For metallic structures, the most commonly investigated defect types include corrosion and fatigue cracking. Applications include the thinning of plates due to corrosion, e.g. at difficult to reach areas such as pipeline supports. Tomography approaches rely on transducers located around the area of interest and changes in the wave pulse arrival time due to thickness reduction (Fig. 5). This requires a dispersive guided wave mode, where the velocity changes with thickness in the frequency range of interest, but not too significantly to completely alter the wave propagation characteristics. In particular, the S_0 mode in a frequency-thickness range below 2 MHz mm has been used for tomography applications (Malyarenko and Hinders 2000), as at low frequency-thickness product it has the highest group velocity, i.e., the fastest arrival time. For single defects of simple geometry, a good match of the estimated and actual thickness reduction was found (Leonard, Malyarenko et al. 2002). For more complex or deep defect geometries or sharp edges, additional effects due to scattering have to be considered and can make accurate sizing challenging. Different reconstruction algorithms and guided wave modes have been investigated for their suitability and compared for specific thickness reductions (Zhao, Royer et al. 2011). Higher wave modes with shorter wavelength due to the higher excitation frequency offer better sensitivity for shallow defects, but less accurate depth sizing of deep defects was found. In general, good results for the detection and localization of corrosion thinning using guided wave tomography have been reported, but accurate sizing can be more complicated depending on the defect type and severity.

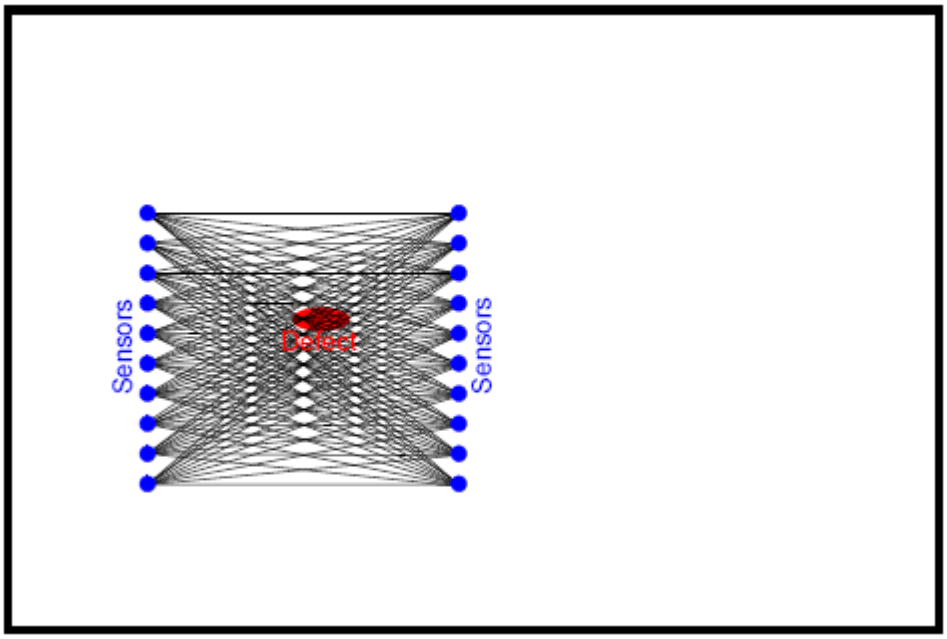

Figure 5. Schematic of Tomography on plate, sensors, wave paths and defect marked.

Significant work has been reported on the first symmetrical Lamb wave mode S_0 and the lowest shear mode SH_0, as their displacement, stress distribution, and propagation velocity at low frequencies are similar to the bulk ultrasonic wave modes and non-dispersive (Zhao and Rose 2004). The wave propagation characteristics are similar to the torsional and longitudinal modes often employed for pipe applications, and for thin wall thickness compared to the pipe diameter locally similar defect sensitivity was observed. The scattering at part and through thickness notches and cracks oriented along and perpendicular to the wave propagation direction was studied experimentally and from FE simulations. Significant variations depending on the defect depth and length relative to the wavelength were found (Demma, Cawley et al. 2003).

The interactions with damage as well as the appropriate damage monitoring strategy were investigated (Lee and Staszewski 2007). For fatigue crack detection, the scattering at cracks emanating from circular cavities (holes) was investigated. The scattering at holes in a plate was studied analytically for flexural waves (A_0 mode) (Pao and Chao 1964), (Fromme and Sayir 2002), and for the S_0 mode (McKeon and Hinders 1999), (Diligent, Grahn et al. 2002), to establish a baseline. (Fromme and Sayir 2002) investigated the changes to the scattered field during fatigue crack growth and found good agreement of experimental results with numerical predictions. Guided waves were employed to successfully detect defects at difficult to reach locations around a hole (Doherty and Chiu 2012) and fatigue cracks emanating at fasteners within a lap joint (Cho and Lissenden 2012). The scattering behavior of guided waves at complete and partial through-thickness notches (Lowe and Diligent 2002), (Fromme and Rouge 2011), and cracks (Chang and Mal 1999) has been predicted and validated experimentally.

As for aerospace structures the areas of high stress concentration are typically known, higher frequency guided waves offer a potential trade-off between smaller monitoring range and improved sensitivity for small defects. Higher frequency guided wave modes have been increasingly used for improved defect detection over shorter distances, as the ratio of the

wavelength to the defect size determines the detection sensitivity. Compared to the lower frequency, fundamental Lamb modes, experimentally the selective excitation of specific modes is more complicated but allows for easier interpretation of results. Finite element simulations combined with modal decomposition were used to study the interaction of Lamb waves with defects for frequency-thickness products up to 5 MHz mm (Terrien, Osmont et al. 2007). High frequency Lamb waves at about 15 MHz mm and the application for crack detection was demonstrated (Greve, Zheng et al. 2008). The detection of fatigue cracks and other defects using the high frequency fundamental Lamb wave modes (Chan, Masserey et al. 2015, Masserey and Fromme 2017), the A_1 mode (Khalili and Cawley 2016), and higher order mode clusters (HOMC) (Ratnam, Balasubramaniam et al. 2012) were demonstrated.

For flat structures, guided wave arrays (Fig. 6a) have been employed (Li and Rose 2001), (Salas and Cesnik 2009). (Wilcox, Lowe et al. 2005) developed a compact, moveable guided wave phased array system using electromagnetic acoustics transducers (EMATs) to excite and receive the S_0 mode. With post-processing similar to conventional ultrasonic phased arrays or in the wavenumber-frequency domain (Wilcox 2003), defects in a metallic plate could be localized. Similar concepts were developed by (Fromme, Wilcox et al. 2006) for the A_0 mode, but employing a circular array of bonded piezoelectric sensors. Different types of defects such as partial and through holes and plate thinning similar to corrosion were successfully detected. The influence of the number and pattern of the sensors on the sidebands and thus selectivity for defect detection were studied (Wilcox, Lowe et al. 2005), (Yu and Giurgiutiu 2012). The sensitivity for defect detection has been improved by employing different signal processing methods (Velichko and Wilcox 2008).

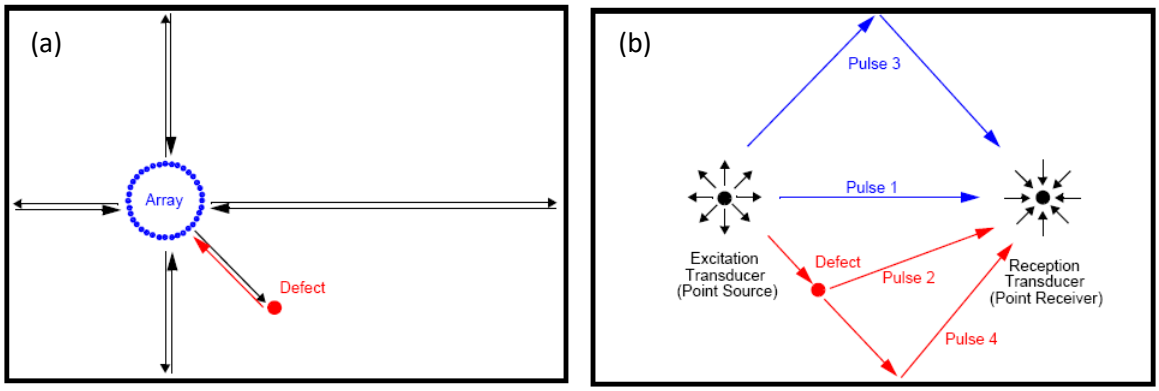

Figure 6. a) Schematic of Localized Array; b) Schematic Pulses Distributed Array.

As localized phased array type transducers have limited sensitivity for defects (cracks) aligned radially to the sensor location, distributed guided wave sensor arrays (Fig. 6b) were investigated (Wang, Rose et al. 2004) (Michaels 2008). Such approaches using permanently bonded sensors are at the cross-over between NDE and Structural Health Monitoring (SHM), often also called Structural Integrity Monitoring (SIM). The main advantage of permanently attached transducers is the reduction of variability if a baseline subtraction approach is employed, which is often necessary to distinguish between reflections at structural features and developing defects, especially for more complex structures (Attarian, Cegla et al. 2014). Damage localization is achieved using the differenced signals (baseline subtraction) to separate scattered signals from structural features and damage. Different signal processing algorithms have been implemented and tested, ranging from elliptical imaging (Wang, Rose et al. 2004)

to more advanced methods, such as minimum variance imaging (Hall, Fromme et al. 2014), maximum-likelihood estimation (Flynn, Todd et al. 2011), and sparse reconstruction (Levine and Michaels 2013). Guided wave imaging algorithms have the potential for damage characterization, as the defect geometry influences the scattering pattern, which can be taken into account to determine likely defect shape and orientation, e.g. for minimum variance imaging (Hall, Fromme et al. 2014).

However, environmental effects such as temperature changes, surface conditions, and loading can affect the arrival time of different signal components and thus the accuracy of the baseline subtraction (Konstantinidis, Drinkwater et al. 2006), (Lu and Michaels 2009), (Chen, Michaels et al. 2012), limiting the effective dynamic range and thus sensitivity. Improvements can be achieved with more advanced signal processing algorithms or corrections for benevolent variations of the baseline, e.g. optimum baseline subtraction and baseline stretching (Croxford, Moll et al. 2010).

3.2 Multi-layered plates, stiffeners, and lap-joints

For complex structures consisting of multiple metallic layers, often connected using sealant layers and fasteners for aerospace applications, or bonded stiffeners and lap joints, the wave propagation and scattering characteristics are typically more complex than for single metallic layers. Taking as an example a structure consisting of two aluminum layers with a sealant layer as a simplified model for aircraft structures, the guided wave mode shapes through the thickness become more complex. Similarities to single layered structures exist, but the fundamental guided waves (not strictly Lamb waves) at low frequencies now consist of the individual bending of the metallic layers (Kostson and Fromme 2009), either in-phase to give a dominant out-of-plane displacement similar to the A_0 Lamb mode or out-of-phase with a predominant in-plane displacement (Fig. 7). Higher order guided wave mode shapes tend to be even more complex and depend significantly on the frequency, geometry, and material properties.

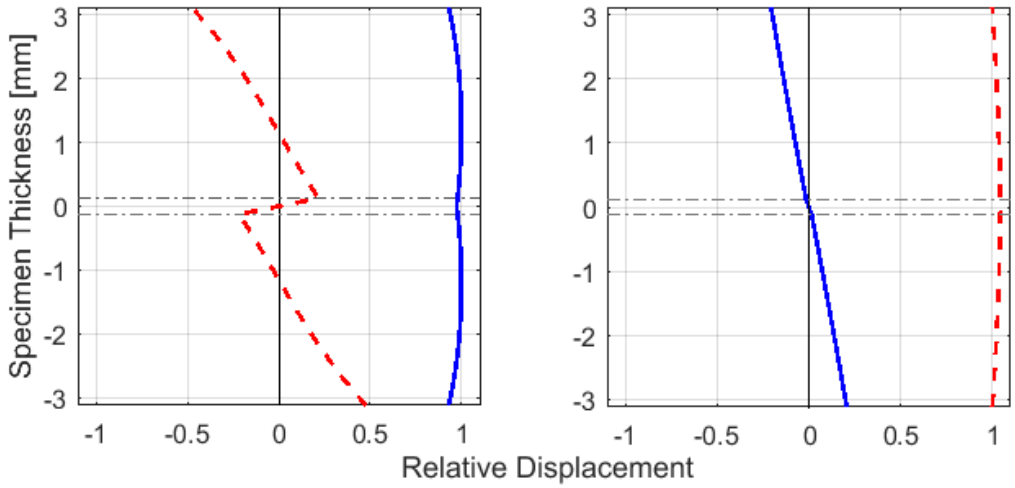

Figure 7. Mode shapes for multi-layer structure (3 mm aluminum, 0.25 mm epoxy, 3 mm aluminum), 100 kHz frequency; a) anti-symmetric mode; b) symmetric mode; solid: out-of-plane; dashed: in-plane displacement.

Lower frequency guided wave modes in multi-layered structures can be considered in analogy to single metal plates and good propagation distances have been achieved (Dalton, Cawley et

al. 2001), as the attenuation due to the sealant layer is typical at acceptable levels. As the guided wave modes have energy distributed through the complete specimen thickness, defect detection is possible even in areas with lack of sealant, but the wave propagation characteristics are influenced by the local contact conditions. The flexural wave mode has been employed to detect and monitor fatigue crack growth adjacent to a fastener hole (Kostson and Fromme 2009), and innovative approaches such as instrumented fasteners (Rakow and Chang 2012) have been proposed. Suitable modes of high frequency guided waves for the inspection of different layers of multi-layered structures can be found employing a mode-tuning technique (Quarry 2004). For multi-layered aircraft structures high frequency guided wave modes have been shown to be sensitive for the detection of manufactured notches (Lindgren, Aldrin et al. 2007), and fatigue cracks (Chan, Masserey et al. 2015), but propagation distances are limited due to attenuation and a proper understanding of the wave propagation characteristics is required.

Bonded stiffeners are widely employed in aerospace structures, contributing in a complex assembly with the aircraft skin and the airframe, to provide strength and stiffness. Adhesive bonding achieves a continuous bond and results in good stiffness and force transfer with relatively low stresses. The quality of the adhesive bonds between aircraft skin and stiffener are important for the structural performance (Di Scalea, Matt et al. 2007). Problems include poor adhesion and inadequate strength of the adhesive material caused by incorrect curing (Thompson and Thompson 1991). The velocity of bulk ultrasonic waves in the adhesive material, which depends to a large degree on material stiffness, may be used to monitor curing of the adhesive (Rokhlin, Hefets et al. 1981), (Freemantle and Challis 1998), (Dixon, Jaques et al. 2004).

Guided waves can be used to monitor continuous bond lines, if their propagation is sensitive to the properties of the bond. This idea has been employed for adhesive joints of parallel plates using Lamb and interface waves (Mal, Xu et al. 1989), (Nagy and Adler 1989). Different possible guided wave modes are reviewed in (Lowe and Cawley 1994). The adhesive thickness and properties influence the guided wave propagation characteristics. Viscoelastic adhesives contribute to the attenuation of the higher order guided wave modes in multi-layered plate structures (Seifried, Jacobs et al. 2002). (Nagy and Adler 1989) used guided waves to inspect adhesive joints between plates. Guided waves propagating in a plate structure can be used in a different configuration to interrogate attachments, e.g. spar on skin (Di Scalea, Matt et al. 2007) or repair patch on skin (Le Crom and Castaings 2010), (Puthillath and Rose 2010).Wave modes guided along a structural feature such as a weld or bonded stiffener have been considered. Trapped modes can exist, e.g. due to the geometry leading to a lower phase velocity than in the surrounding plate, concentrating energy at the feature and thus enabling long distance propagation. This has been demonstrated for the case of a butt weld between two plates (local thickness increase) for a partially-trapped compression-like mode (Sargent 2006) and a perfectly-trapped shear-like mode with very little dispersion (Fan and Lowe 2009), (Castaings and Lowe 2008). These wave modes can be employed to inspect the weld material and the material in the heat-affected zone (HAZ). Shear modes propagating along a stiffener have been used to monitor the curing of the bond line to a plate structure (Fan, Castaings et al. 2013).

3.3 Anisotropic structures, composites

Anisotropic and inhomogeneous materials are widely employed, e.g. carbon or glass fiber reinforced pre-preg composites for aircraft structures and wind turbine blades, as they offer improved strength to weight ratios. The degree of anisotropy depends strongly on the material, e.g. unidirectional composites have stronger anisotropy than cross-ply or quasi-isotropic lay-ups. Typically material properties are less well known than for metallic materials and might vary within the structure due to manufacturing imperfections. Guided wave propagation characteristics can be predicted using a global matrix approach such as implemented in the Disperse software (Pavlakovic, Lowe et al. 1997) or a transfer matrix approach (Hosten and Castaings 1993). The anisotropy has a strong effect on the S_0 guided wave mode, as its velocity depends on the in-plane stiffness. E.g. for a unidirectional plate, the S_0 phase and group velocities in the fiber direction can be a factor 3 higher than perpendicular to the fiber orientation. The effect on the anti-symmetric A_0 mode is lower, as the flexural wave mode depends as well on the properties of the matrix material (Fig. 8).

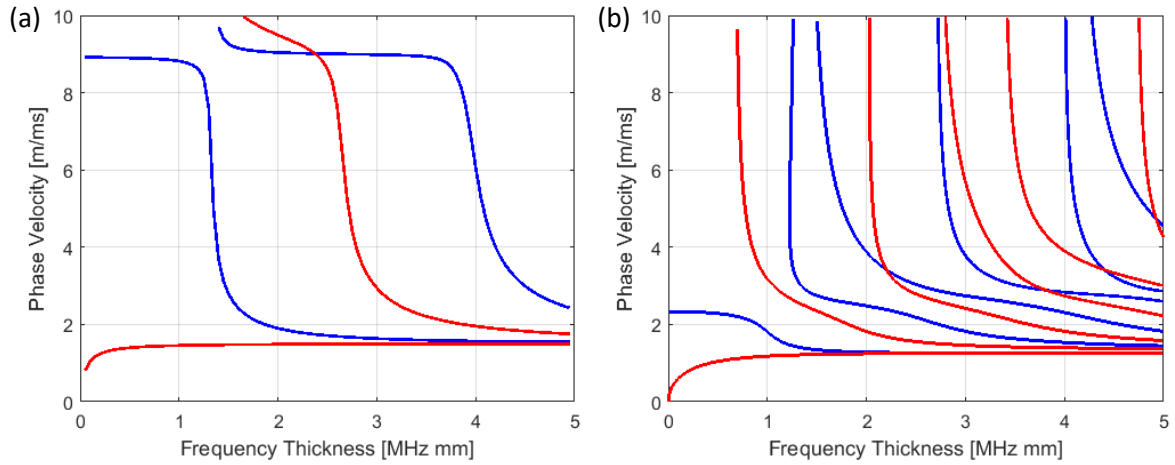

Figure 8. Dispersion diagram for unidirectional composite plate; a) wave propagation in fiber direction; b) perpendicular to fiber direction.

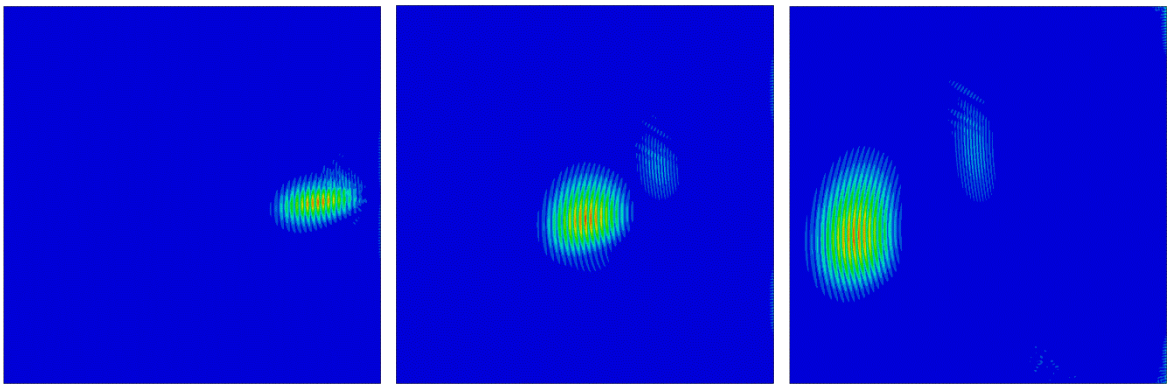

Figure 9. Finite Element simulation of S_0 guided wave mode propagation in monocrystalline silicon (0.38 mm thickness, 5 MHz frequency); showing wave skew relative to horizontal direction of wave excitation at three time points.

In the non-principal directions the S_0 and SH_0 wave modes are coupled and the SH_0 mode can exhibit cusps, complicating the wave propagation. Furthermore, wave skewing in the non-

principal directions occurs for all wave modes, depending on the degree of anisotropy (Fig. 9). The skew angle describes the different directions of the phase and energy (group) velocities and can be calculated from the anisotropic material properties. Energy focusing along the fiber directions occurs, which can further complicate measurements. (Chapuis, Terrien et al. 2010) investigated the energy radiation of Lamb waves in a thin fiber reinforced composite plate. Numerical and experimental results showed a significant direction-dependent focusing effect of the Lamb modes. Higher amplitudes and higher propagation speed along the fiber direction of a unidirectional composite plate is shown in Fig. 10. Group velocity curves in thin anisotropic, carbon fiber-reinforced epoxy laminates were measured using a point-source point-receiver configuration and compared to theoretical curves (Veidt and Sachse 1994). The influence of the anisotropy on Zero Group Velocity (ZGV) Lamb modes was investigated in monocrystalline silicon wafers using a line laser source (Prada, Clorennec et al. 2009). For an incident ultrasonic beam on an anisotropic multilayered structure, (Potel, Baly et al. 2005) demonstrated that the Lamb wave beam generated in the plate can deviate with respect to the sagittal plane of excitation towards the stiffer direction of the anisotropic structure. (Leleux, Micheau et al. 2013) developed a multi-element matrix ultrasonic probe to inspect large composite plate components in pulse-echo mode from one single position and detect delamination and impact damage.

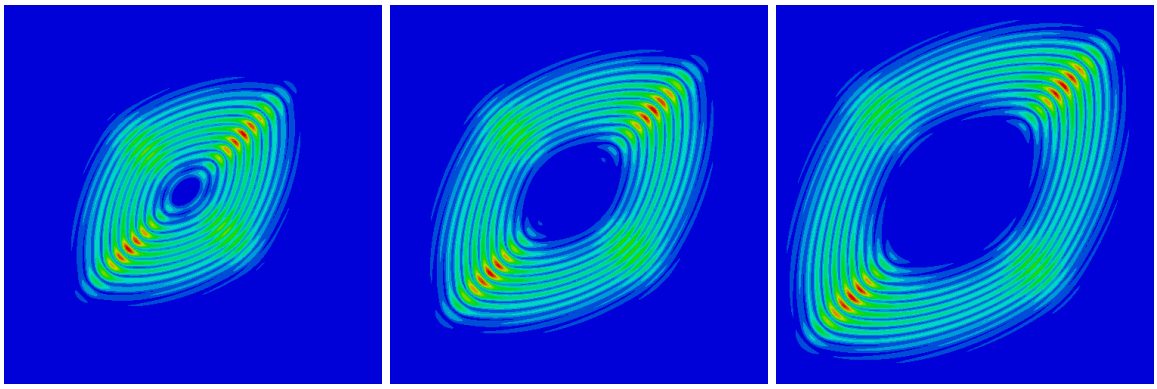

Figure 10. Finite Element simulation of A_0 guided wave mode propagation in 45 degree unidirectional composite (3.6 mm thickness, 100 kHz frequency) at three time points.

The propagation of guided waves is complicated due to the anisotropic and inhomogeneous properties of the composites (Castaings and Hosten 2003). Together with typically high attenuation values, this makes monitoring and inspection using higher guided wave modes difficult and only limited work has been reported (Su, Ye et al. 2006). In general, it has been found advantageous to operate with a single wave mode at low frequency in order to avoid complications in the signal analysis and high attenuation. The fundamental symmetric mode S_0 at low frequency has limited dispersion and the fastest propagation velocity, but the velocity depends strongly on the propagation direction relative to the composite layup fiber direction and the S_0 mode is typically coupled with the SH_0 mode (Datta and Shah 2009). It was found that the S_0 mode is not sensitive to delaminations between plies being under zero shear stress condition (Guo and Cawley 1993).

For carbon and glass fiber composite materials the critical damage mechanisms differ from metals. Manufacturing defects such as porosity, in- and out-of-plane weaving, fiber misalignment can be inherent even in new composite structure and might necessitate acceptance inspection before service. Important in-service defects include high and low

velocity impact damage, which can lead to varying damage mechanisms such as matrix and fiber breakage, matrix cracks, and delamination. The scattering of guided waves at a composite delamination is complex (Ng and Veidt 2011). The fundamental anti-symmetric mode A_0 has a shorter wavelength than the S_0 mode (Grondel, Paget et al. 2002) and thus in principle better sensitivity for defect detection. Furthermore, the directionality of the wave propagation characteristics is significantly less dependent on the anisotropic material properties, leading to similar velocities in all directions for quasi-isotropic and cross-ply (0/90) layups (Datta and Shah 2009). The A_0 guided wave mode has been employed to detect different types of damage, such as cracking, fatigue and delaminations in composite structures (Castaings, Singh et al. 2012). The A_0 mode tends to be more sensitive to delaminations than the S_0 mode and can detect delaminations at any depth (Guy, Jayet et al. 2003). Mode conversion from the A_0 to S_0 mode was observed when the guided wave interferes with the delamination boundaries (Ramadas, Balasubramaniam et al. 2010), confirmed from experimental work (Kazys, Demcenko et al. 2006). Delaminations can in principle be located by estimating the propagation speed and time of flight from the reflected signal. Separate reflections from the delamination edges appear when the delamination length increases (relative to the wavelength). Composites subjected to impact damage were investigated (Kundu, Das et al. 2008), (Diamanti, Hodgkinson et al. 2004). The scattered wave amplitude pattern around a delamination showed a large forward scattered wave relative to the reflected pulse (Ng and Veidt 2011). (Mesnil, Leckey et al. 2014) investigated the energy trapping in a delamination area. Guided wave approaches have been proposed for the rapid inspection of silicon wafers to detect small cracks that increase wafer breakage rates. (Chakrapani, Padiyar et al. 2012) used air-coupled transducers in pitch-catch configuration to generate the fundamental antisymmetric Lamb wave mode A_0 in thin mono- and polycrystalline silicon wafers and detect cracks.

3.4 Curved Structures

While the theoretical derivations above were developed for flat plates, in industrial applications often curved structures exist. The limitations of the applicability of concepts developed for flat plates has been investigated (Gridin, Craster et al. 2003), and it was found that the incurred error is typically low as long as the radius of curvature is significantly larger than the plate thickness. Therefore, most curved structures such as aircraft skins or tank walls can in good approximation be tested similar to plates. Within limitations this is also possible when localized wave propagation in large diameter, thin-walled pipelines is considered, e.g. around the circumference or along the length of the pipe (Liu and Qu 1998, Zhao and Rose 2004). Circumferential guided waves have been employed to detect localized corrosion damage (Howard and Cegla 2017) or coating disbonds (Van Velsor, Rose et al. 2009).

4. Pipes

Guided waves have been successfully employed for the nondestructive testing and monitoring of pipelines, with several commercially available testing equipment systems (Rose 2002), (Mudge 2001), (Alleyne, Jones et al. 2017), (Vinogradov, Eason et al. 2018). Several international norms have been established for guided wave testing of pipelines (e.g. BS 9690-2:2011, ASTM E2775 – 16, ASTM E2929 - 13). Pipes can be considered as one-dimensional structures along which the energy of axisymmetric guided ultrasonic wave modes propagates with little loss of energy, and propagation distances of up to 100 meters have been achieved

(Cawley, Lowe et al. 2003). One of the main initial obstacles was the controlled excitation and reception of selected axisymmetric guided wave modes, as even at low frequency, multiple modes can be present. A typical dispersion diagram for a pipe is shown in Fig. 11. Modes are typically grouped as longitudinal (L), flexural (F), or torsional (T), with the number of nodes along the circumference and thickness labelled, e.g. the lowest longitudinal mode L(0,1) with uniform displacement around the circumference.

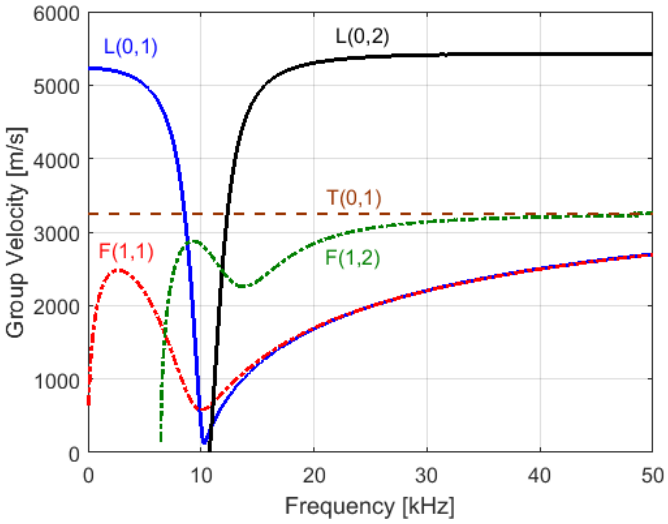

Figure 11. Dispersion diagram of group velocity for 6 inch, schedule 40 steel pipe; only lowest torsional mode T(0,1), flexural modes F(1,1) and F(1,2), and longitudinal modes L(0,1) and L(0,2) shown.

Much of the early work employed the longitudinal mode L(0,2), as it has very limited dispersion and the fastest group velocity and thus earliest arrival time. Similarly, the torsional mode T(0,1) has been widely used for nondestructive testing, as it exhibits no dispersion and can be considered equivalent to the shear-horizontal (SH) mode in plates. For buried and coated pipes or liquid loading, attenuation increases depending on the viscosity and mode shape, limiting the achievable inspection distances and detection sensitivity. Viscoelastic coating is often used to insulate pipes and can lead to high attenuation, causing problems for guided wave testing. Care must be taken to select specific guided wave modes and excitation frequencies to obtain low attenuation and thus good propagation distances (Barshinger and Rose 2004). For pipes buried in sand, the attenuation increases depending on the excitation frequency, water saturation, and soil compaction (Leinov, Lowe et al. 2015). Both the L(0,2) and T(0,1) mode have uniform stress and displacement around the circumference (no nodes) and the wave propagation can be considered as one-dimensional along the pipe, making analysis of the results and correlation to defect location along the pipe length straightforward. Typically, this is expressed as a percentage of the cross-sectional area (CSA), but allows only limited localization around the pipe circumference and classification of defect shape and type. Even for uncoated, above surface pipes, periodic welds and flanges between different sections of pipe act as reflectors and mostly uniform reflection around the circumference is received, which can be used to calibrate defect sensitivity. Depending on the employed guided wave mode and the geometry of the defect, e.g. circumferential or axial orientation of cracks, corrosion pitting, the reflection and mode conversion depending on the extent, shape, and depth can be predicted (Cho, Hongerholt et al. 1997, Bai, Shah et al. 2001, Ratassepp, Fletcher et al. 2010, Lovstad and Cawley 2012).

Synthetic focusing, based on post-processing of individual transducer signals, allows the improvement of defect imaging and localization. Different approaches for guided wave focusing were developed (Hayashi, Kawashima et al. 2005, Davies and Cawley 2009). The propagation of guided waves around pipe elbows poses a problem to achieve monitoring of the complete pipe volume at the bend and beyond. For detection of corrosion and erosion, especially the outside region of the bend can be difficult to monitor, as waves tend to travel the shortest distance around the inside of the bend. Monitoring systems (Brath, Simonetti et al. 2017) and focusing of non-axisymmetric modes (Rose, Zhang et al. 2005) have been proposed, together with modelling to correct for pulse distortion (Sanderson, Hutchins et al. 2013). Long-term monitoring using permanently fixed electro-magnetic acoustic transducers (EMAT) can help to improve the sensitivity for small defects (Herdovics and Cegla 2018).

Similarities exist with rail applications, where efficient monitoring can be achieved by guided wave propagation along the rail. Dispersion curves and mode shapes are rather complicated due to the rail cross section (Hayashi, Song et al. 2003) (Bartoli, Marzani et al. 2006), but dominant propagating modes with energy in the different sections of the rail can be identified and propagation along the rail achieved (Cawley, Lowe et al. 2003). Monitoring systems to automatically detect rail breakage over long distances (km) have been developed (Loveday 2012). Accurate and repeatable experimental excitation and reception of specific guided wave modes is required to achieve good signal-to-noise ratio (SNR) for the detection of small defects.

5. Experimental methods

Guided wave measurements typically require different transducers and experimental equipment compared to standard bulk ultrasonic pulse-echo and pitch-catch measurements. As discussed briefly in section 2, guided waves are multi-modal and dispersive, and measurements are often conducted at excitation frequencies in the kHz range below the cut-off frequencies of higher wave modes. Therefore, often the aim is to achieve selective experimental excitation of a specific guided wave mode with good control of the time signal and thus frequency content.

For higher frequency guided wave applications (typically in the lower MHz range) standard ultrasonic equipment and transducers can be employed (Fig. 12). However, in the kHz frequency range often employed in guided wave testing, the choice of transducers available from commercial manufacturers is more limited, in parts due to physical restrictions on the design of resonant piezoelectric transducers. For a number of applications, simple (and cheap) piezoelectric elements, dry-coupled or glued to the specimen have been employed for guided wave measurements (Fig. 12). The element size and coupling influence the excited guided wave mode, as described e.g. by (Yu and Giurgiutiu 2012). Often measurements are conducted with a fixed excitation location using a permanently bonded piezoelectric element to allow comparison to theoretical configurations and to allow baseline subtraction. As the employed transducers are often non-resonant, the excitation time signal can be prescribed, e.g. as a narrow frequency bandwidth sinusoid (Fig. 4), by synthesizing the voltage signal using an arbitrary function generator. Using a voltage or power amplifier with the required frequency bandwidth, high excitation amplitudes with good signal-to-noise ratio (SNR) can be achieved. Typical approaches can be found in literature, e.g. (Lowe, Alleyne et al. 1998, Giurgiutiu, Zagrai et al. 2002, Fromme, Wilcox et al. 2006).

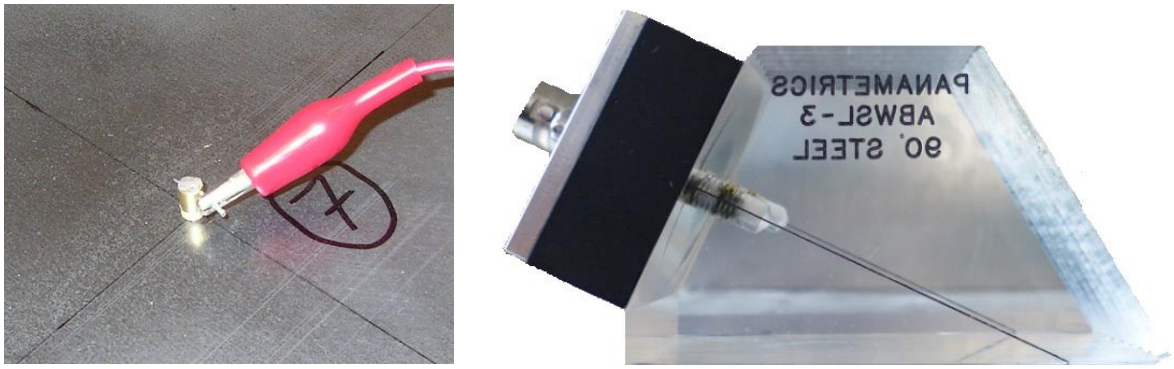

Figure 12. Picture of permanently bonded piezoelectric disc (with backing mass) and wedge transducer.

For phased or distributed arrays, piezoelectric elements have been used with good success to monitor large structures. However, for long term monitoring, especially at higher temperatures and challenging environmental conditions, degradation of the bond layer used to couple the transducers and thus changes to the signals can occur (Attarian, Cegla et al. 2014). For a number of applications noncontact excitation and measurement methods have advantages, such as the lack of a coupling medium and possibility to scan the transducer along the structure.

Air-coupled transducers have been developed and are commercially available, either using a membrane or piezoelectric/static element. Controlling the angle and thus wavelength projection on the specimen, selective excitation of guided wave modes is possible (Castaings and Hosten 2008). Air-coupled excitation has a better efficiency for mode shapes with a significant out-of-plane component, but as the acoustic impedance of air and metals is significantly different, the overall excitation efficiency is limited.

Electromagnetic acoustic transducers (EMAT) allow for the non-contact excitation and reception of guided ultrasonic waves (Hirao and Ogi 2017). Typically, a static magnetic field is applied by a permanent magnet and an eddy current induced by an alternating current in a wire coil located close to the conductive specimen surface (Kawashima 1976). The interaction of the magnetic field and current generates a Lorentz force, which is perpendicular to both the magnetic field and eddy current. If the specimen material is ferromagnetic, in addition to the Lorentz force, magnetostrictive effects lead to induced stress and thus wave excitation of significantly increased amplitude (Jian, Dixon et al. 2006). The usage of EMATs is described in guidelines such as the ASTM E1774-96 Standard Guide for Electromagnetic Acoustic Transducers.

EMATs do not require couplant, and thus are suitable for elevated temperatures, automated scanning and guided wave excitation is not directly affected by surface roughness and coating. The wire coil to induce eddy currents can easily be designed to generate specific patterns, e.g. a meander or racetrack style coil to prescribe the wavelength of the excited wave mode. As the generated stresses are perpendicular to the magnetic field and eddy current (Fig. 13), EMATs are well suited to excite guided wave modes with a significant in-plane component, e.g. shear horizontal (SH) waves. Limitations exist as the induced eddy currents depend on the stand-off distance and frequency. The skin depth of the eddy current density is inversely proportional to the frequency of the alternating current. For typical guided wave testing frequencies, the skin depth is less than 1 mm in steel. This limits the excitation amplitude for higher frequencies and thick specimens. A large current is required to obtain high amplitudes, requiring specialized

electronic equipment such as power amplifiers and limiting the usage for explosion restricted applications. EMATs typically require strong magnets such as rare earth magnets, e.g. neodymium-boron, but could also employ electromagnets. The magnitude of the magnetostrictive effect depends on the specific material properties and can vary significantly, e.g. between different steel alloys. For sensors that target specifically the magnetostrictive effect, materials with controlled properties such as nickel or iron cobalt can be bonded to the structure, e.g. as a sleeve around pipes or with liquid couplant to allow rotation of a directional sensor (Vinogradov, Eason et al. 2018).

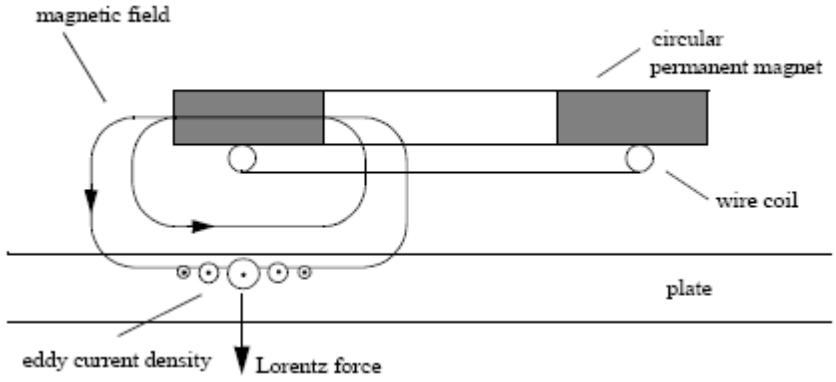

Figure 13. Diagram of EMAT for excitation of A_0 guided wave mode in plate with radially magnetized circular permanent magnet, wire coil and Lorentz force due to induced eddy current shown schematically.

Lasers provide another non-contact excitation and measurement method widely used for laboratory studies (Zhang, Krishnaswamy et al. 2006), (Park, An et al. 2014), but due to safety constraints are more difficult to employ for field measurements. Typically, a pulsed laser beam is used to locally heat the material with the resulting thermal stresses exciting guided waves. Care must be taken to avoid too high laser intensity leading to material ablation. As most excitation lasers are class III or IV, the relevant safety precautions must be observed. The laser beam can be optically shaped to achieve specific patterns and the pulse repetition rate can be matched to the required guided wave excitation frequency. However, as the excitation process relies on thermal processes with time delays mostly restricted to the specimen surface, exact control of the guided wave time signal and mode shape can be difficult to achieve.

Commercial laser interferometers or vibrometers (Fig. 14) exist that allow the pointwise measurement of guided waves with very good accuracy (Fromme and Sayir 2002, Staszewski, Lee et al. 2007). The out-of-plane component of the specimen surface motion can be easily measured and quantified using either the phase interference to measure displacement or frequency shift to measure surface velocity. While instruments exist to measure in-plane motion directly, the repeatability and accuracy is typically lower than for out-of-plane measurement. As such, laser measurements of guided waves in plates have been used more widely for the A_0 (flexural) mode with a significant out-of-plane (bending) motion, but the measurement of out-of-plane component of the S_0 mode on untreated surfaces is also possible (Fromme, Pizzolato et al. 2018). Using surface treatment (e.g. retro-reflective tape) and measurements with laser beams at 3 different angles, all 3 surface motion components can be quantified (Staszewski, Lee et al. 2007). Often either the laser interferometer or specimen are

scanned relative to each other to measure guided wave propagation and scattering with good spatial accuracy to either quantify propagation speeds and thus material characteristics or detailed scattering patterns at defects. This methodology together with fixed piezoelectric excitation has been employed often, as it is well suited to the specific characteristics of guided waves and allows for comparison to predictions using numerical simulations.

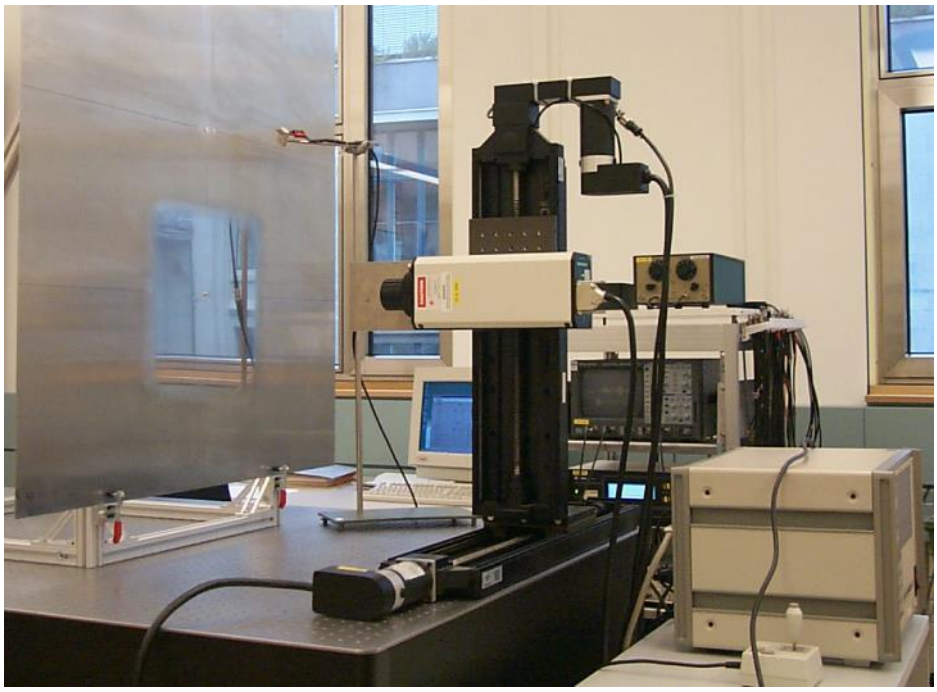

Figure 14. Photograph of laser vibrometer mounted on scanning rig.

6. Simulations

For the understanding of guided wave propagation and scattering at defects, numerical simulations are useful to predict the behavior and understand phenomena better. Apart from theoretical calculations for simple geometries, different numerical methods with their respective advantages and drawbacks have been widely used. The most widely used method is Finite Element Analysis (FEA), as commercial software packages can be employed for computations. Other methods such as the Finite Difference Method (FDM), Boundary Elements, and peridynamic modelling have respective advantages, typically improved computational efficiency but often only limited standard, commercial software is available. The Semi-Analytical Finite Element (SAFE) method allows for the efficient computation of guided wave propagation along structures with irregular cross-sections and can be combined with local numerical approaches for the hybrid modelling of scattering, reflection, and transmission of guided waves.

A range of commercial FEA software packages, but also open-source programs (Huthwaite 2014) can be used to simulate guided wave propagation and scattering. Both explicit time marching and implicit schemes can be employed. Especially for implicit schemes, absorbing layers remove unwanted boundary reflections and allow smaller, more computationally efficient models to be used (Drozdz, Moreau et al. 2006, Rajagopal, Drozdz et al. 2012, Shen

and Giurgiutiu 2015). Stability criteria require small elements compared to the wavelength and short time steps for explicit time integration. For the long propagation distances achievable with guided waves, this leads to large numbers of required elements and degrees of freedom. Depending on the NDE problem, 2D simulations of a cross-section of the structure can provide valuable insights with significant faster computation times. 2D FE models of wave propagation and scattering in composites to characterize impact damage have been developed (Pol and Banerjee 2013). The anisotropic material properties of composites can easily be implemented in commercial FE software and used in 3D FE models to study the scattering at delamination in composites (Murat, Khalili et al. 2016), (Ng, Veidt et al. 2012). Different approaches for approximation of the damage using either Cartesian or adapted meshes can be used.

In order to efficiently predict guided wave propagation in complex wave guide geometries, e.g., stiffener bonded to a plate, the SAFE (Semi-Analytical Finite Element) method uses a 2D FE discretization of the cross-section of the waveguide, in combination with an analytical description of the behavior in the direction along the waveguide (Castaings and Lowe 2008). This significantly reduces the computational effort and has proven useful for irregularly-shaped waveguides such as rails (Damljanovic and Weaver 2004). SAFE simulations can be conducted using flexible commercial or proprietary FE codes. Different implementations can be used, e.g. by (Predoi, Castaings et al. 2007), extended for complex propagating modes (Castaings and Lowe 2008) to allow for energy leakage. The dispersion diagram can be calculated by solving the eigenvalue solutions over the frequency range, to find the complex wavenumber, attenuation, and mode shape for each frequency.

SAFE methods for the guided wave propagation along waveguides can be combined with local FE or other numerical methods to calculate the scattering at localized defects and the reflected and transmitted wave modes (Jezzine, Imperiale et al. 2018). Such hybrid models are computationally efficient but require care to achieve accurate coupling of the computational domains. Hybrid FE methods (Rose 2017) were used to study the scattering of guided waves at a hole (Paskaramoorthy, Shah et al. 1989) and to compare to experiments for the scattering of the fundamental S_0 mode at a hole with a crack (Chang and Mal 1999). Hybrid boundary element methods were used to study Lamb wave reflection and mode conversion at a plate edge above the lowest cut-off frequency (Cho and Rose 1996). Hybrid FE modelling combined with the local interaction simulation approach (LISA) can be extended to allow for material anisotropy and damping (Shen and Cesnik 2016).

Finite Difference (FD) simulations based on a displacement formulation of the wave equations in isotropic, linear elastic media were used to study the scattering of guided waves (Harker 1984). (Virieux 1986) presented a two-dimensional, stress-velocity FD formulation for modelling bulk wave propagation in heterogeneous media. The formulation was based on a system of first-order hyperbolic equations discretized on a staggered grid. This type of grid, first proposed by Madariaga (Madariaga 1976), has the useful property to minimize the number of variables per grid cell. A 3D displacement-velocity FD formulation was used to investigate the scattering of high frequency guided waves at cracks emanating from a fastener hole (Masserey and Fromme 2017). The Elastodynamic Finite Integration Technique (EFIT) (Fellinger, Marklein et al. 1995) uses a similar formulation. The complex 3D geometry of

impact damage in composites was implemented from X-ray computed tomography scans and the interaction of guided waves investigated (Leckey, Rogge et al. 2014). For composites, the performance compared to different commercial FE solvers and experimental results was compared (Leckey, Wheeler et al. 2018). Other numerical methodologies such as the time domain spectral element method (Ostachowicz, Kudela et al. 2012) and peri-ultrasound (Hafezi, Alebrahim et al. 2017) have been employed to simulate guided wave propagation and scattering.

7. Summary

The application of guided waves for non-destructive testing and monitoring has progressed significantly over the last decades. As guided waves are dispersive and multi-modal, a good understanding of the wave propagation and defect interaction in the structure of interest is required to ensure reliable defect detection and sensitivity. For the testing of pipelines, several commercially successful systems exist, allowing for the testing of pipe sections up to 100 meters from a single access location and providing advantages over other NDE systems for a range of applications. However, the range of guided waves is more limited for coated structures and can be complicated for plate structures, requiring adaptation to the specific inspection problem and often numerical simulations to gain a full understanding of the wave physics. Specialized transducer and electronic equipment, often in the kHz frequency range, is required for the generation and reception of guided waves. Good control over the guided wave mode and directionality helps to improve sensitivity for the detection of small defects. Further steps to gain widespread acceptance will require advanced simulations to quantify sensitivity and demonstrate applicability for complex industrial structures under real-life conditions.

8. References

Achenbach, J. D. (1973). Wave Propagation in Elastic Solids. Amsterdam, Elsevier Science.

Alleyne, D. and P. Cawley (1991). "A 2-DIMENSIONAL FOURIER-TRANSFORM METHOD FOR THE MEASUREMENT OF PROPAGATING MULTIMODE SIGNALS." Journal of the Acoustical Society of America **89**(3): 1159-1168.

Alleyne, D., R. Jones and T. Vogt (2017). "GW Test An Introduction to Long-Range Screening Using Guided Waves." Materials Evaluation **75**(10): 1206-1213.

Attarian, V. A., F. B. Cegla and P. Cawley (2014). "Long-term stability of guided wave structural health monitoring using distributed adhesively bonded piezoelectric transducers." Structural Health Monitoring-an International Journal **13**(3): 265-280.

Auld, B. A. (1973). Acoustic Fields and Waves in Solids. Hoboken, John Wiley and Sons.

Bai, H., A. H. Shah, N. Popplewell and S. K. Datta (2001). "Scattering of guided waves by circumferential cracks in steel pipes." Journal of Applied Mechanics-Transactions of the Asme **68**(4): 619-631.

Barshinger, J. N. and J. L. Rose (2004). "Guided wave propagation in an elastic hollow cylinder coated with a viscoelastic material." IEEE Transactions on Ultrasonics, Ferroelectrics, and Frequency Control **51**(11): 1547-1556.

Bartoli, I., A. Marzani, F. Lanza di Scalea and E. Viola (2006). "Modeling wave propagation in damped waveguides of arbitrary cross-section." Journal of Sound and Vibration **295**(3-5): 685-707.

Brath, A. J., F. Simonetti, P. B. Nagy and G. Instanes (2017). "Guided Wave Tomography of Pipe Bends." Ieee Transactions on Ultrasonics Ferroelectrics and Frequency Control **64**(5): 847-858.

Castaings, M. and B. Hosten (2003). "Guided waves propagating in sandwich structures made of anisotropic, viscoelastic, composite materials." Journal of the Acoustical Society of America **113**(5): 2622-2634.

Castaings, M. and B. Hosten (2008). "Ultrasonic guided waves for health monitoring of high-pressure composite tanks." Ndt & E International **41**(8): 648-655.

Castaings, M. and M. Lowe (2008). "Finite element model for waves guided along solid systems of arbitrary section coupled to infinite solid media." Journal of the Acoustical Society of America **123**(2): 696-708.

Castaings, M., D. Singh and P. Viot (2012). "Sizing of impact damages in composite materials using ultrasonic guided waves." Ndt & E International **46**: 22-31.
Cawley, P., M. J. S. Lowe, D. N. Alleyne, B. Pavlakovic and P. D. Wilcox (2003). "Practical long range guided wave testing: applications to pipes and rail." Materials Evaluation **61**(1): 66-74.
Chakrapani, S. K., M. J. Padiyar and K. Balasubramaniam (2012). "Crack Detection in Full Size Cz-Silicon Wafers Using Lamb Wave Air Coupled Ultrasonic Testing (LAC-UT)." Journal of Nondestructive Evaluation **31**(1): 46-55.
Chan, H., B. Masserey and P. Fromme (2015). "High frequency guided ultrasonic waves for hidden fatigue crack growth monitoring in multi-layer model aerospace structures." Smart Materials and Structures **24**(2).
Chang, Z. S. and A. Mal (1999). "Scattering of Lamb waves from a rivet hole with edge cracks." Mechanics of Materials **31**(3): 197-204.
Chapuis, B., N. Terrien and D. Royer (2010). "Excitation and focusing of Lamb waves in a multilayered anisotropic plate." Journal of the Acoustical Society of America **127**(1): 198-203.
Chen, X., J. E. Michaels, S. J. Lee and T. E. Michaels (2012). "Load-differential imaging for detection and localization of fatigue cracks using Lamb waves." Ndt & E International **51**: 142-149.
Cho, H. and C. J. Lissenden (2012). "Structural health monitoring of fatigue crack growth in plate structures with ultrasonic guided waves." Structural Health Monitoring-an International Journal **11**(4): 393-404.
Cho, Y. H., D. D. Hongerholt and J. L. Rose (1997). "Lamb wave scattering analysis for reflector characterization." Ieee Transactions on Ultrasonics Ferroelectrics and Frequency Control **44**(1): 44-52.
Cho, Y. H. and J. L. Rose (1996). "A boundary element solution for a mode conversion study oil the edge reflection of Lamb waves." Journal of the Acoustical Society of America **99**(4): 2097-2109.
Croxford, A. J., J. Moll, P. D. Wilcox and J. E. Michaels (2010). "Efficient temperature compensation strategies for guided wave structural health monitoring." Ultrasonics **50**(4-5): 517-528.
Dalton, R. P., P. Cawley and M. J. S. Lowe (2001). "The potential of guided waves for monitoring large areas of metallic aircraft fuselage structure." Journal of Nondestructive Evaluation **20**(1): 29-46.
Damljanovic, V. and R. L. Weaver (2004). "Propagating and evanescent elastic waves in cylindrical waveguides of arbitrary cross section." Journal of the Acoustical Society of America **115**(4): 1572-1581.
Datta, S. K. and A. H. Shah (2009). Elastic Waves in Composite Media and Structures With Applications to Ultrasonic Nondestructive Evaluation Introduction. Elastic Waves in Composite Media and Structures: With Applications to Ultrasonic Nondestructive Evaluation**:** 1-9.
Davies, J. and P. Cawley (2009). "The Application of Synthetic Focusing for Imaging Crack-Like Defects in Pipelines Using Guided Waves." Ieee Transactions on Ultrasonics Ferroelectrics and Frequency Control **56**(4): 759-771.
Demma, A., P. Cawley and M. Lowe (2003). "Scattering of the fundamental shear horizontal mode from steps and notches in plates." Journal of the Acoustical Society of America **113**(4): 1880-1891.
Di Scalea, F. L., H. Matt, I. Bartoli, S. Coccia, G. Park and C. Farrar (2007). "Health monitoring of UAV wing skin-to-spar joints using guided waves and macro fiber composite transducers." Journal of Intelligent Material Systems and Structures **18**(4): 373-388.
Diamanti, K., J. M. Hodgkinson and C. Soutis (2004). "Detection of low-velocity impact damage in composite plates using lamb waves." Structural Health Monitoring-an International Journal **3**(1): 33-41.
Diligent, O., T. Grahn, A. Bostrom, P. Cawley and M. J. S. Lowe (2002). "The low-frequency reflection and scattering of the S-0 Lamb mode from a circular through-thickness hole in a plate: Finite Element, analytical and experimental studies." Journal of the Acoustical Society of America **112**(6): 2589-2601.
Dixon, S., D. Jaques, S. B. Palmer and G. Rowlands (2004). "The measurement of shear and compression waves in curing epoxy adhesives using ultrasonic reflection and transmission techniques simultaneously." Measurement Science and Technology **15**(5): 939-947.
Doherty, C. and W. K. Chiu (2012). "Scattering of ultrasonic-guided waves for health monitoring of fuel weep holes." Structural Health Monitoring-an International Journal **11**(1): 27-42.
Drozdz, M., L. Moreau, M. Castaings, M. J. S. Lowe and P. Cawley (2006). Efficient numerical modelling of absorbing regions for boundaries of guided waves problems. Review of Progress in Quantitative Nondestructive Evaluation, Vols 25a and 25b. D. O. Thompson and D. E. Chimenti. Melville, Amer Inst Physics. **820:** 126-133.
Fan, Z., M. Castaings, M. J. S. Lowe, C. Biateau and P. Fromme (2013). "Feature-guided waves for monitoring adhesive shear modulus in bonded stiffeners." NDT and E International **54**: 96-102.
Fan, Z. and M. J. S. Lowe (2009). "Elastic waves guided by a welded joint in a plate." Proceedings of the Royal Society a-Mathematical Physical and Engineering Sciences **465**(2107): 2053-2068.
Fellinger, P., R. Marklein, K. J. Langenberg and S. Klaholz (1995). "NUMERICAL MODELING OF ELASTIC-WAVE PROPAGATION AND SCATTERING WITH EFIT - ELASTODYNAMIC FINITE INTEGRATION TECHNIQUE." Wave Motion **21**(1): 47-66.

Flynn, E. B., M. D. Todd, P. D. Wilcox, B. W. Drinkwater and A. J. Croxford (2011). "Maximum-likelihood estimation of damage location in guided-wave structural health monitoring." Proceedings of the Royal Society a-Mathematical Physical and Engineering Sciences **467**(2133): 2575-2596.
Freemantle, R. J. and R. E. Challis (1998). "Combined compression and shear wave ultrasonic measurements on curing adhesive." Measurement Science and Technology **9**(8): 1291-1302.
Fromme, P., M. Pizzolato, J. L. Robyr and B. Masserey (2018). "Lamb wave propagation in monocrystalline silicon wafers." Journal of the Acoustical Society of America **143**(1): 287-295.
Fromme, P. and C. Rouge (2011). "Directivity of guided ultrasonic wave scattering at notches and cracks C3 - Journal of Physics: Conference Series." **269**(1).
Fromme, P. and M. B. Sayir (2002). "Detection of cracks at rivet holes using guided waves." Ultrasonics **40**(1-8): 199-203.
Fromme, P. and M. B. Sayir (2002). "Measurement of the scattering of a Lamb wave by a through hole in a plate." Journal of the Acoustical Society of America **111**(3): 1165-1170.
Fromme, P., P. D. Wilcox, M. J. S. Lowe and P. Canvley (2006). "On the development and testing of a guided ultrasonic wave array for structural integrity monitoring." Ieee Transactions on Ultrasonics Ferroelectrics and Frequency Control **53**(4): 777-785.
Fromme, P., P. D. Wilcox, M. J. S. Lowe and P. Cawley (2006). "On the development and testing of a guided ultrasonic wave array for structural integrity monitoring." IEEE Transactions on Ultrasonics, Ferroelectrics, and Frequency Control **53**(4): 777-784.
Giurgiutiu, V., A. Zagrai and J. J. Bao (2002). "Piezoelectric Wafer Embedded Active Sensors for Aging Aircraft Structural Health Monitoring." Structural Health Monitoring-an International Journal **1**(1): 41-61.
Graff, K. F. (1975). Wave Motion in Elastic Solids. New York, Oxford University Press.
Greve, D. W., P. Zheng and I. J. Oppenheim (2008). "The transition from Lamb waves to longitudinal waves in plates." Smart Materials & Structures **17**(3).
Gridin, D., R. V. Craster, J. Fong, M. J. S. Lowe and M. Beard (2003). "The high-frequency asymptotic analysis of guided waves in a circular elastic annulus." Wave Motion **38**(1): 67-90.
Grondel, S., C. Paget, C. Delebarre, J. Assaad and K. Levin (2002). "Design of optimal configuration for generating A(0) Lamb mode in a composite plate using piezoceramic transducers." Journal of the Acoustical Society of America **112**(1): 84-90.
Guo, N. and P. Cawley (1993). "THE INTERACTION OF LAMB WAVES WITH DELAMINATIONS IN COMPOSITE LAMINATES." Journal of the Acoustical Society of America **94**(4): 2240-2246.
Guy, P., Y. Jayet and L. Goujon (2003). Guided waves interaction with complex delaminations. Application to damage detection in composite structures. Smart Nondestructive Evaluation and Health Monitoring of Structural and Biological Systems Ii. T. Kundu. **5047:** 25-33.
Hafezi, M. H., R. Alebrahim and T. Kundu (2017). "Peri-ultrasound for modeling linear and nonlinear ultrasonic response." Ultrasonics **80**: 47-57.
Hall, J. S., P. Fromme and J. E. Michaels (2014). "Guided Wave Damage Characterization via Minimum Variance Imaging with a Distributed Array of Ultrasonic Sensors." Journal of Nondestructive Evaluation **33**(3): 299-308.
Harker, A. H. (1984). "Numerical modelling of the scattering of elastic waves in plates." Journal of Nondestructive Evaluation **4**(2): 89-106.
Hayashi, T., K. Kawashima, Z. Q. Sun and J. L. Rose (2005). "Guided wave focusing mechanics in pipe." Journal of Pressure Vessel Technology-Transactions of the Asme **127**(3): 317-321.
Hayashi, T., W. J. Song and J. L. Rose (2003). "Guided wave dispersion curves for a bar with an arbitrary cross-section, a rod and rail example." Ultrasonics **41**(3): 175-183.
Herdovics, B. and F. Cegla (2018). "Structural health monitoring using torsional guided wave electromagnetic acoustic transducers." Structural Health Monitoring-an International Journal **17**(1): 24-38.
Hirao, M. and H. Ogi (2017). Brief Instruction to Build EMATs. Electromagnetic Acoustic Transducers: Noncontacting Ultrasonic Measurements Using Emats, 2nd Edition. Tokyo, Springer Japan**:** 69-79.
Hosten, B. and M. Castaings (1993). "TRANSFER-MATRIX OF MULTILAYERED ABSORBING AND ANISOTROPIC MEDIA - MEASUREMENTS AND SIMULATIONS OF ULTRASONIC WAVE-PROPAGATION THROUGH COMPOSITE-MATERIALS." Journal of the Acoustical Society of America **94**(3): 1488-1495.
Howard, R. and F. Cegla (2017). "Detectability of corrosion damage with circumferential guided waves in reflection and transmission." Ndt & E International **91**: 108-119.
Huthwaite, P. (2014). "Accelerated finite element elastodynamic simulations using the GPU." Journal of Computational Physics **257**: 687-707.
Jezzine, K., A. Imperiale, E. Demaldent, F. Le Bourdais, P. Calmon and N. Dominguez (2018). Modeling approaches for the simulation of ultrasonic inspections of anisotropic composite structures in the CIVA software

platform. 44th Annual Review of Progress in Quantitative Nondestructive Evaluation, Vol 37. D. E. Chimenti and L. J. Bond. Melville, Amer Inst Physics. **1949**.
Jian, X., S. Dixon, R. S. Edwards and J. Morrison (2006). "Coupling mechanism of an EMAT." Ultrasonics **44**: E653-E656.
Kawashima, K. (1976). "EXPERIMENTS WITH 2 TYPES OF ELECTROMAGNETIC ULTRASONIC TRANSDUCERS." Journal of the Acoustical Society of America **60**(2): 365-373.
Kazys, R., A. Demcenko, E. Zukauskas and L. Mazeika (2006). "Air-coupled ultrasonic investigation of multi-layered composite materials." Ultrasonics **44**: E819-E822.
Khalili, P. and P. Cawley (2016). "Excitation of Single-Mode Lamb Waves at High-Frequency-Thickness Products." Ieee Transactions on Ultrasonics Ferroelectrics and Frequency Control **63**(2): 303-312.
Konstantinidis, G., B. W. Drinkwater and P. D. Wilcox (2006). "The temperature stability of guided wave structural health monitoring systems." Smart Materials & Structures **15**(4): 967-976.
Kostson, E. and P. Fromme (2009). "Fatigue crack growth monitoring in multi-layered structures using guided ultrasonic waves." Journal of Physics: Conference Series **195**.
Kundu, T., S. Das, S. A. Martin and K. V. Jata (2008). "Locating point of impact in anisotropic fiber reinforced composite plates." Ultrasonics **48**(3): 193-201.
Le Crom, B. and M. Castaings (2010). "Shear horizontal guided wave modes to infer the shear stiffness of adhesive bond layers." Journal of the Acoustical Society of America **127**(4): 2220-2230.
Leckey, C. A. C., M. D. Rogge and F. R. Parker (2014). "Guided waves in anisotropic and quasi-isotropic aerospace composites: Three-dimensional simulation and experiment." Ultrasonics **54**(1): 385-394.
Leckey, C. A. C., K. R. Wheeler, V. N. Hafiychuk, H. Hafiychuk and D. A. Timucin (2018). "Simulation of guided-wave ultrasound propagation in composite laminates: Benchmark comparisons of numerical codes and experiment." Ultrasonics **84**: 187-200.
Lee, B. C. and W. J. Staszewski (2007). "Lamb wave propagation modelling for damage detection: II. Damage monitoring strategy." Smart Materials & Structures **16**(2): 260-274.
Leinov, E., M. J. S. Lowe and P. Cawley (2015). "Investigation of guided wave propagation and attenuation in pipe buried in sand." Journal of Sound and Vibration **347**: 96-114.
Leleux, A., P. Micheau and M. Castaings (2013). "Long Range Detection of Defects in Composite Plates Using Lamb Waves Generated and Detected by Ultrasonic Phased Array Probes." Journal of Nondestructive Evaluation **32**(2): 200-214.
Leonard, K. R., E. V. Malyarenko and M. K. Hinders (2002). "Ultrasonic Lamb wave tomography." Inverse Problems **18**(6): 1795-1808.
Levine, R. M. and J. E. Michaels (2013). "Model-based imaging of damage with Lamb waves via sparse reconstruction." Journal of the Acoustical Society of America **133**(3): 1525-1534.
Li, J. and J. L. Rose (2001). "Implementing guided wave mode control by use of a phased transducer array." Ieee Transactions on Ultrasonics Ferroelectrics and Frequency Control **48**(3): 761-768.
Lindgren, E., J. C. Aldrin, K. Jata, B. Scholes and J. Knopp (2007). Ultrasonic plate waves for fatigue crack detection in multi-layered metallic structures. Health Monitoring of Structural and Biological Systems 2007. T. Kundu. **6532**.
Liu, G. L. and J. M. Qu (1998). "Guided circumferential waves in a circular annulus." Journal of Applied Mechanics-Transactions of the Asme **65**(2): 424-430.
Loveday, P. W. (2012). "Guided Wave Inspection and Monitoring of Railway Track." Journal of Nondestructive Evaluation **31**(4): 303-309.
Lovstad, A. and P. Cawley (2012). "The reflection of the fundamental torsional mode from pit clusters in pipes." Ndt & E International **46**: 83-93.
Lowe, M. J. S., D. N. Alleyne and P. Cawley (1998). "The mode conversion of a guided wave by a part-circumferential notch in a pipe." Journal of Applied Mechanics-Transactions of the Asme **65**(3): 649-656.
Lowe, M. J. S. and P. Cawley (1994). "The applicability of plate wave techniques for the inspection of adhesive and diffusion bonded joints." Journal of Nondestructive Evaluation **13**(4): 185-200.
Lowe, M. J. S. and O. Diligent (2002). "Low-frequency reflection characteristics of the s(0) Lamb wave from a rectangular notch in a plate." Journal of the Acoustical Society of America **111**(1): 64-74.
Lu, Y. and J. E. Michaels (2009). "Feature Extraction and Sensor Fusion for Ultrasonic Structural Health Monitoring Under Changing Environmental Conditions." Ieee Sensors Journal **9**(11): 1462-1471.
Madariaga, R. (1976). "DYNAMICS OF AN EXPANDING CIRCULAR FAULT." Bulletin of the Seismological Society of America **66**(3): 639-666.
Mal, A. K., P. C. Xu and Y. Barcohen (1989). "ANALYSIS OF LEAKY LAMB WAVES IN BONDED PLATES." International Journal of Engineering Science **27**(7): 779-791.
Malyarenko, E. V. and M. K. Hinders (2000). "Fan beam and double crosshole Lamb wave tomography for mapping flaws in aging aircraft structures." Journal of the Acoustical Society of America **108**(4): 1631-1639.

Masserey, B. and P. Fromme (2017). "Analysis of high frequency guided wave scattering at a fastener hole with a view to fatigue crack detection." Ultrasonics **76**: 78-86.
McKeon, J. C. P. and M. K. Hinders (1999). "Lamb wave scattering from a through hole." Journal of Sound and Vibration **224**(5): 843-862.
Mesnil, O., C. A. C. Leckey and M. Ruzzene (2014). Instantaneous wavenumber estimation for damage quantification in layered plate structures. Health Monitoring of Structural and Biological Systems 2014. T. Kundu. **9064**.
Michaels, J. E. (2008). "Detection, localization and characterization of damage in plates with an in situ array of spatially distributed ultrasonic sensors." Smart Materials & Structures **17**(3).
Michaels, J. E., S. J. Lee, A. J. Croxford and P. D. Wilcox (2013). "Chirp excitation of ultrasonic guided waves." Ultrasonics **53**(1): 265-270.
Mudge, P. J. (2001). "Field application of the Teletest (R) long-range ultrasonic testing technique." Insight **43**(2): 74-77.
Murat, B. I. S., P. Khalili and P. Fromme (2016). "Scattering of guided waves at delaminations in composite plates." Journal of the Acoustical Society of America **139**(6): 3044-3052.
Nagy, P. B. and L. Adler (1989). "NONDESTRUCTIVE EVALUATION OF ADHESIVE JOINTS BY GUIDED-WAVES." Journal of Applied Physics **66**(10): 4658-4663.
Ng, C.-T. and M. Veidt (2011). "Scattering of the fundamental anti-symmetric Lamb wave at delaminations in composite laminates." Journal of the Acoustical Society of America **129**(3): 1288-1296.
Ng, C. T., M. Veidt, L. R. F. Rose and C. H. Wang (2012). "Analytical and finite element prediction of Lamb wave scattering at delaminations in quasi-isotropic composite laminates." Journal of Sound and Vibration **331**(22): 4870-4883.
Ostachowicz, W., P. Kudela, M. Krawczuk and A. Zak (2012). Guided Waves in Structures for SHM: The Time-Domain Spectral Element Method. Oxford, Blackwell Science Publ.
Pao, Y. H. and C. C. Chao (1964). "DIFFRACTIONS OF FLEXURAL WAVES BY A CAVITY IN AN ELASTIC PLATE." Aiaa Journal **2**(11): 2004-2010.
Park, B., Y. K. An and H. Sohn (2014). "Visualization of hidden delamination and debonding in composites through noncontact laser ultrasonic scanning." Composites Science and Technology **100**: 10-18.
Paskaramoorthy, R., A. H. Shah and S. K. Datta (1989). "SCATTERING OF FLEXURAL WAVES BY CAVITIES IN A PLATE." International Journal of Solids and Structures **25**(10): 1177-1191.
Pavlakovic, B., M. Lowe, D. Alleyne and P. Cawley (1997). Disperse: A general purpose program for creating dispersion curves.
Pol, C. B. and S. Banerjee (2013). "Modeling and analysis of propagating guided wave modes in a laminated composite plate subject to transient surface excitations." Wave Motion **50**(5): 964-978.
Potel, C., S. Baly, J. F. de Belleval, M. Lowe and P. Gatignol (2005). "Deviation of a monochromatic Lamb wave beam in anisotropic multilayered media: Asymptotic analysis, numerical and experimental results." Ieee Transactions on Ultrasonics Ferroelectrics and Frequency Control **52**(6): 987-1001.
Prada, C., D. Clorennec, T. W. Murray and D. Royer (2009). "Influence of the anisotropy on zero-group velocity Lamb modes." Journal of the Acoustical Society of America **126**(2): 620-625.
Predoi, M. V., M. Castaings, B. Hosten and C. Bacon (2007). "Wave propagation along transversely periodic structures." Journal of the Acoustical Society of America **121**(4): 1935-1944.
Puthillath, P. and J. L. Rose (2010). "Ultrasonic guided wave inspection of a titanium repair patch bonded to an aluminum aircraft skin." International Journal of Adhesion and Adhesives **30**(7): 566-573.
Quarry, M. J. (2004). Guided wave inspection of multi-layered structures.
Rajagopal, P., M. Drozdz, E. A. Skelton, M. J. S. Lowe and R. V. Craster (2012). "On the use of absorbing layers to simulate the propagation of elastic waves in unbounded isotropic media using commercially available Finite Element packages." Ndt & E International **51**: 30-40.
Rakow, A. and F.-K. Chang (2012). "A structural health monitoring fastener for tracking fatigue crack growth in bolted metallic joints." Structural Health Monitoring-an International Journal **11**(3): 253-267.
Ramadas, C., K. Balasubramaniam, M. Joshi and C. V. Krishnamurthy (2010). "Interaction of guided Lamb waves with an asymmetrically located delamination in a laminated composite plate." Smart Materials & Structures **19**(6).
Ratassepp, M., S. Fletcher and M. J. S. Lowe (2010). "Scattering of the fundamental torsional mode at an axial crack in a pipe." Journal of the Acoustical Society of America **127**(2): 730-740.
Ratnam, D., K. Balasubramaniam and B. W. Maxfield (2012). "Generation and Detection of Higher-Order Mode Clusters of Guided Waves (HOMC-GW) Using Meander-Coil EMATs." Ieee Transactions on Ultrasonics Ferroelectrics and Frequency Control **59**(4): 727-737.
Rokhlin, S. I., M. Hefets and M. Rosen (1981). "AN ULTRASONIC INTERFACE-WAVE METHOD FOR PREDICTING THE STRENGTH OF ADHESIVE BONDS." Journal of Applied Physics **52**(4): 2847-2851.

Rose, J. L. (2002). "A baseline and vision of ultrasonic guided wave inspection potential." Journal of Pressure Vessel Technology-Transactions of the Asme **124**(3): 273-282.
Rose, J. L. (2002). "Standing on the shoulders of giants: An example of guided wave inspection." Materials Evaluation **60**(1): 53-59.
Rose, J. L. (2014). Ultrasonic Guided Waves in Solid Media. Cambridge, Cambridge Univ Press.
Rose, J. L. (2017). "Aspects of a Hybrid Analytical Finite Element Method Approach for Ultrasonic Guided Wave Inspection Design." Journal of Nondestructive Evaluation, Diagnostics and Prognostics of Engineering Systems **1**(1): 011001-011001-011010.
Rose, J. L., L. Zhang, M. J. Avioli and P. J. Mudge (2005). "A natural focusing low frequency guided wave experiment for the detection of defects beyond elbows." Journal of Pressure Vessel Technology-Transactions of the Asme **127**(3): 310-316.
Salas, K. I. and C. E. S. Cesnik (2009). "Guided wave excitation by a CLoVER transducer for structural health monitoring: theory and experiments." Smart Materials & Structures **18**(7).
Sanderson, R. M., D. A. Hutchins, D. R. Billson and P. J. Mudge (2013). "The investigation of guided wave propagation around a pipe bend using an analytical modeling approach." Journal of the Acoustical Society of America **133**(3): 1404-1414.
Sargent, J. P. (2006). "Corrosion detection in welds and heat-affected zones using ultrasonic Lamb waves." Insight **48**(3): 160-167.
Seifried, R., L. J. Jacobs and J. M. Qu (2002). "Propagation of guided waves in adhesive bonded components." Ndt & E International **35**(5): 317-328.
Shen, Y. F. and C. E. S. Cesnik (2016). "Hybrid local FEM/global LISA modeling of damped guided wave propagation in complex composite structures." Smart Materials and Structures **25**(9): 20.
Shen, Y. F. and V. Giurgiutiu (2015). "Effective non-reflective boundary for Lamb waves: Theory, finite element implementation, and applications." Wave Motion **58**: 22-41.
Staszewski, W. J., B. C. Lee and R. Traynor (2007). "Fatigue crack detection in metallic structures with Lamb waves and 3D laser vibrometry." Measurement Science and Technology **18**(3): 727-739.
Su, Z., L. Ye and Y. Lu (2006). "Guided Lamb waves for identification of damage in composite structures: A review." Journal of Sound and Vibration **295**(3-5): 753-780.
Terrien, N., D. Osmont, D. Royer, F. Lepoutre and A. Deom (2007). "A combined finite element and modal decomposition method to study the interaction of Lamb modes with micro-defects." Ultrasonics **46**(1): 74-88.
Thompson, R. B. and D. O. Thompson (1991). "PAST EXPERIENCES IN THE DEVELOPMENT OF TESTS FOR ADHESIVE BOND STRENGTH." Journal of Adhesion Science and Technology **5**(8): 583-599.
Van Velsor, J. K., J. L. Rose and J. B. Nestleroth (2009). "Enhanced Coating Disbond Detection Capabilities in Pipe Using Circumferential Shear Horizontal Guided Waves." Materials Evaluation **67**(10): 1179-1188.
Veidt, M. and W. Sachse (1994). "ULTRASONIC POINT-SOURCE POINT-RECEIVER MEASUREMENTS IN THIN SPECIMENS." Journal of the Acoustical Society of America **96**(4): 2318-2326.
Velichko, A. and P. D. Wilcox (2008). "Guided wave arrays for high resolution inspection." Journal of the Acoustical Society of America **123**(1): 186-196.
Viktorov, I. A. (1967). Rayleigh and Lamb waves - Physical Theory and Applications New York, Plenum.
Vinogradov, S., T. Eason and M. Lozev (2018). "Evaluation of Magnetostrictive Transducers for Guided Wave Monitoring of Pressurized Pipe at 200 degrees C." Journal of Pressure Vessel Technology-Transactions of the Asme **140**(2): 7.
Virieux, J. (1986). "P-SV-WAVE PROPAGATION IN HETEROGENEOUS MEDIA - VELOCITY-STRESS FINITE-DIFFERENCE METHOD." Geophysics **51**(4): 889-901.
Wang, C. H., J. T. Rose and F. K. Chang (2004). "A synthetic time-reversal imaging method for structural health monitoring." Smart Materials & Structures **13**(2): 415-423.
Wilcox, P. D. (2003). "A rapid signal processing technique to remove the effect of dispersion from guided wave signals." Ieee Transactions on Ultrasonics Ferroelectrics and Frequency Control **50**(4): 419-427.
Wilcox, P. D., M. Lowe and P. Cawley (2005). "Omnidirectional guided wave inspection of large metallic plate structures using an EMAT array." Ieee Transactions on Ultrasonics Ferroelectrics and Frequency Control **52**(4): 653-665.
Yu, L. and V. Giurgiutiu (2012). "Piezoelectric Wafer Active Sensors in Lamb Wave-Based Structural Health Monitoring." Jom **64**(7): 814-822.
Zhang, F., S. Krishnaswamy and C. M. Lilley (2006). "Bulk-wave and guided-wave photoacoustic evaluation of the mechanical properties of aluminum/silicon nitride double-layer thin films." Ultrasonics **45**(1-4): 66-76.
Zhao, X., R. L. Royer, S. E. Owens and J. L. Rose (2011). "Ultrasonic Lamb wave tomography in structural health monitoring." Smart Materials & Structures **20**(10): 10.
Zhao, X. L. and J. L. Rose (2004). "Guided circumferential shear horizontal waves in an isotropic hollow cylinder." Journal of the Acoustical Society of America **115**(5): 1912-1916.

Zhao, X. L. and J. L. Rose (2004). Three-dimensional defect in a plate boundary element modeling for guided wave scattering. Advances in Nondestructive Evaluation, Pt 1-3. S. S. Lee, D. J. Yoon, J. H. Lee and S. Lee. **270-273:** 453-460.